

Structures, Electronic Properties, Spectroscopies and Hexagonal Monolayer Phase of a Family of Unconventional Fullerenes $C_{64}X_4$

$$(X = H, F, Cl, Br)$$

Qing-Bo Yan, Qing-Rong Zheng, and Gang Su*

College of Physical Sciences, Graduate University of Chinese Academy of Sciences,

P.O. Box 4588, Beijing 100049, China

Abstract

A systematic first-principles study within density functional theory on the geometrical structures and electronic properties of unconventional fullerene C_{64} and its derivatives $C_{64}X_4$ ($X = H, F, Cl, Br$) has been performed. By searching through all 3465 isomers of C_{64} , the ground state of C_{64} is found to be spherical shape with D_2 symmetry, which differs from the parent cage of the recently synthesized $C_{64}H_4$ that is pear-shaped with C_{3v} symmetry. We found that the addition of the halogen atoms like F, Cl, Br to the pentagon-pentagon fusion vertex of C_{64} cage could enhance the stability, forming the unconventional fullerenes $C_{64}X_4$. The Mulliken charge populations, LUMO-HOMO gap energies and density of states are calculated, showing that different halogen atoms added to C_{64} will cause remarkably different charge populations of the $C_{64}X_4$ molecule; the chemical deriving could enlarge the energy gaps and affect the electronic structures distinctly. It is unveiled that $C_{64}F_4$ is even more stable than $C_{64}H_4$, as the C-X bond energy of the former is higher than that of the latter. The computed spectra of $C_{64}H_4$ molecules agree well with the experimental data; the IR, Raman, NMR spectra of $C_{64}X_4$ ($X = F, Cl, Br$) are also calculated to stimulate further experimental investigations. Finally, it is uncovered by total energy calculations that $C_{64}X_4$ could form a stable hexagonal monolayer.

*Author to whom correspondence should be addressed. Email: gsu@gucas.ac.cn

Fullerenes are closed-cage carbon molecules of 12 pentagons and several hexagons. Since discovery of Buckminster fullerene C_{60} [1] in 1985, intensive theoretical and experimental works have been done to study the structures and properties of fullerenes. The conventional fullerenes such as C_{60} , C_{70} , C_{70+2n} , $n = 1, 2, \dots$ are satisfying the empirical isolated pentagon rule (IPR)[2, 3], which states that the most stable fullerenes are those in which every pentagon is surrounded by five hexagons, ensuring the minimum curvature of the fullerene cage (i.e., the minimum strain)[4]. Fullerenes with other number of carbons are impossible to have all the pentagons isolated in the carbon cage, thus they are called unconventional fullerenes or non-IPR fullerenes, which are believed to be labile and difficult to synthesize. In fact, most of the several stable fullerene isomers[5] which had been isolated are satisfying IPR. For applications, fullerenes and their derivatives are potential new agents and materials for molecular electronics, nanoprobe, superconductors, and nonlinear optics. Thus if IPR could be efficiently violated in some ways, the bank of stable fullerenes for practical applications will be much enriched.

In the recent years, it has been uncovered that some non-IPR fullerenes may be stabilized through metallic endohedral ($Sc_2@C_{66}$ [6], $A_xSc_{3-x}N@C_{68}$ [7], $La_2@C_{72}$ [8], etc.). The other effort and progress have also been made in chemical deriving. In 2004, Xie *et al.*[9] had successfully synthesized a new exohedral chemical deriving non-IPR D_{5h} fullerene[50] (say, $C_{50}Cl_{10}$, with 10 chlorine atoms added to the pentagon-pentagon vertex fusions) in milligram by a graphite arc-discharge process modified by introducing a small amount of carbon tetrachloride (CCl_4) in the helium atmosphere. Later, another new chemical deriving non-IPR fullerene[64] (namely, $C_{64}H_4$, with 4 hydrogen atoms added to the vertex of a triplet directly fused pentagons) has been successfully prepared by Wang *et al.*[10] in milligram with similar method. As CCl_4 was added to provide chlorine source in the case of $C_{50}Cl_{10}$, methane (CH_4) was introduced to provide hydrogen for $C_{64}H_4$. Both $C_{50}Cl_{10}$ and $C_{64}H_4$ are stabilized by the chemical modification on the pentagon-pentagon fusion vertex. This clue hints a promising general method to stabilize non-IPR fullerenes. While an efficient and controllable method to prepare the metallic endohedral fullerenes with macroscopic quantity is not yet matured, the chemical deriving might open a useful way to obtain stable non-IPR fullerenes.

Moreover, many questions are still unclear: What is the ground state of C_{64} ? How about the electronic properties? Since the adding atoms in $C_{50}Cl_{10}$ are Cl, what will happen if the H atoms in $C_{64}H_4$ are replaced by other atoms, for instance, F, Cl, Br? Here, by first-

principles density functional calculations, we shall address these issues, and report intensive studies on the geometrical structures, electronic properties and spectroscopies of C_{64} and its derivatives $C_{64}X_4$ ($X = H, F, Cl, Br$). As it is uncovered that $C_{50}Cl_{10}$ molecules could form a hexagonal monolayer [11], we also investigate the possibility that $C_{64}X_4$ could form a hexagonal monolayer. Our present study would deepen understanding of the properties of the recently isolated fulleride $C_{64}H_4$, and could also stimulate further experimental efforts on $C_{64}X_4$ ($X = F, Cl, Br$).

We have generated all of the 3465 topologically distinct isomers of C_{64} cage by spiral algorithm[12], and sorted them by the corresponding pentagon-pentagon adjacency (PPA) numbers. (Definition: one distinct C-C bond shared by two adjacent pentagons in fullerenes is counted as one PPA.) Then, we have calculated the C_{64} isomers with small PPA numbers ($N_{PPA} = 2, 3, 4$) by the semiempirical MNDO method[13]. (see supporting materials.) In Gaussian-like terminology, that would be called MNDO//MNDO calculations, in which $B//A$ represents B level energy calculation based on the geometry optimized on A level. It had been proved that the semiempirical MNDO method could reproduce the ab initio or density functional relative energies of fullerene isomers with useful high accuracy[14, 15].

Among them, nine isomers of C_{64} with the lowest energies (Fig. 1) were chosen, and their derivatives were generated. Using the density functional theory (DFT)[16], we have calculated geometries and relative energies of above nine isomers and their derivatives. In particular, we have invoked the B3LYP functional, which combines the Becke three parameter non-local hybrid exchange potential[17] and the nonlocal correlation functional of Lee-Yang-Parr[18]. The basis set 6-31G* was used in the B3LYP calculations. The B3LYP/6-31G* calculations also give the LUMO-HOMO gaps. The harmonic vibrational frequencies and nuclear magnetic shielding tensors were calculated at the B3LYP/6-31G* and GIAO-B3LYP/6-31G* level, respectively.

All of the calculations are completed by Gaussian 03[19] except that the density of states (DOS) and monolayer total energies of $C_{64}X_4$ are calculated by means of the ABINIT package[20]. This package is coded within the DFT framework based on pseudopotentials and plane waves. Particularly, in our calculations, Troullier-Martins norm conserving pseudopotentials[21] and the Teter parametrization[22] of the Ceperley-Alder exchange-correlation potential were used.

Fig. 1 shows shapes and symmetries of the nine lowest-energy isomers of C_{64} obtained

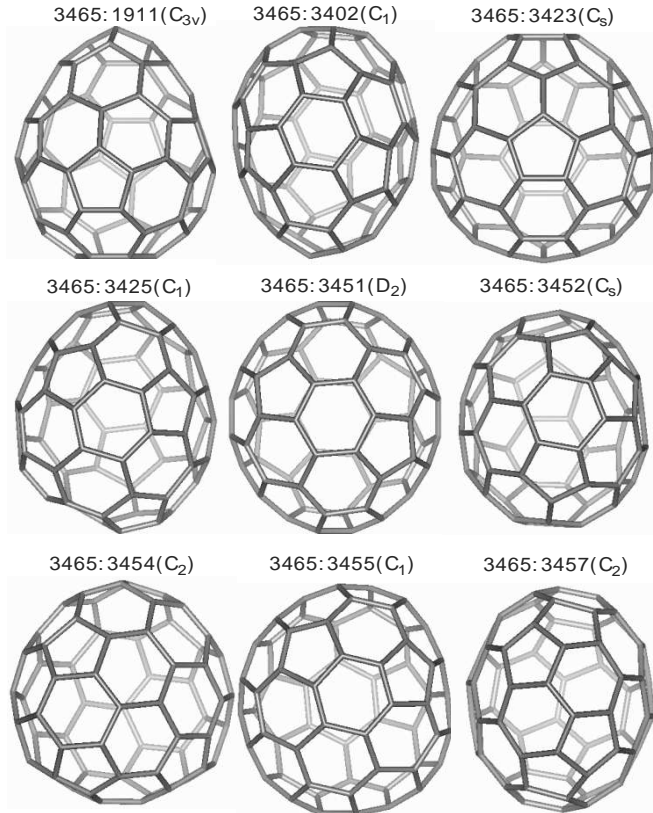


FIG. 1: The 9 lowest-energy isomers of C_{64} obtained at MNDO.

at MNDO level. They have been labeled as 3465 : n , where n denotes the isomer number in spiral nomenclature[12]. We reoptimized the geometries and recalculated their relative energies by B3LYP/6-31G* method, where the LUMO-HOMO gap energies are obtained. The details are listed in Table I.

As seen in Table I, the isomer 3451 (numbering in spiral nomenclature[12]) is the ground state of C_{64} , followed by the isomer 3452 and 3457. The isomer 3451 is nearly spherical shaped, with D_2 symmetry, while the isomer 3452 and 3457 bear C_s and C_2 symmetry, respectively. These three lowest-energy isomers have two pairs of adjacent pentagons (counted as 2-PPA), and the rest isomers with higher energies all have three couples of adjacent pentagons (counted as 3-PPA) except that the isomer 1911, has a triplet of fused pentagons (also counted as 3-PPA). This pear-shaped C_{3v} symmetry isomer 1911, which is just the carbon cage parent of the synthesized $C_{64}H_4$ by Wang *et al.*[10], however, is not apparently favored in energy when it is compared with other eight isomers. The ground state isomer 3451 also has the largest LUMO-HOMO gap energy, followed by the isomer 3457, whereas

TABLE I: MNDO//MNDO, B3LYP/6-31G*//B3LYP/6-31G* relative energies (in eV), LUMO-HOMO gap energies (E_{gap} , in eV) of the nine lowest-energy C_{64} isomers

Isomer ^a	Symm	N_{PPA}^b	N_{PPFV}^c	Relative Energy		E_{gap}
				MNDO ^d	B3LYP ^e	
1 (1911)	C_{3v}	3	4	1.0979 [4]	1.2403 [6]	1.0879
2 (3402)	C_1	3	6	1.4144 [8]	1.4706 [9]	1.4245
3 (3423)	C_s	3	6	1.1597 [6]	1.2156 [5]	1.3845
4 (3425)	C_1	3	6	1.4319 [9]	1.2995 [7]	1.2408
5 (3451)	D_2	2	4	0.0000 [1]	0.0000 [1]	2.2327
6 (3452)	C_s	2	4	0.2600 [2]	0.2987 [2]	2.0482
7 (3454)	C_2	3	6	1.3619 [7]	1.4330 [8]	1.6311
8 (3455)	C_1	3	6	1.1178 [5]	1.1116 [4]	1.9369
9 (3457)	C_2	2	4	0.4807 [3]	0.5563 [3]	1.8547

^aLabeled as m(n) form, where (n) was the numbering in spiral nomenclature[12].

^bNumber of pentagon-pentagon adjacency (PPA).

^cNumber of pentagon-pentagon fusion vertex (PPFV).

^d[n] indicates the stability order on MNDO level.

^e[n] indicates the stability order on B3LYP/6-31G* level.

that of the isomer 1911 is the smallest in the nine.

It may be worth to note that the stability order of the nine isomers obtained by B3LYP/6-31G* calculations is similar, but not exactly the same to that by MNDO. Both methods give the same order for the most stable structures (the isomer 3451, 3452, 3457).

The pentagon-pentagon fusion vertex (PPFV) are usually considered to be the most active sites of the fullerene[23], and the syntheses of stable $C_{50}Cl_{10}$ and $C_{64}H_4$ also clearly evidence that the chemical modification on the PPFV could effectively release the large steric strain of non-IPR fullerenes. Here we attach H and Cl atoms to the PPFV of above nine C_{64} isomers to construct C_{64} fullerene derivatives. As listed in Table I, isomers 1911, 3451, 3452, 3457 have 4 PPFV, while others have 6 PPFV. Thus, the corresponding fullerene derivatives are $C_{64}X_4$ and $C_{64}X_6$ ($X = H$ or Cl), respectively. Since the number of the added X atom is not fixed, the relative energy is not suitable for evaluating the relative stability. In order

TABLE II: B3LYP/6-31G*//B3LYP/6-31G* bond energies ΔE (in eV), LUMO-HOMO gap energies (E_{gap} , in eV) of the derivatives of nine lowest-energy C_{64} isomers

Isomer	n^a	$C_{64}H_n$		$C_{64}Cl_n$	
		$\Delta E(\text{B3LYP})$	E_{gap}	$\Delta E(\text{B3LYP})$	E_{gap}
1(1911)	4	3.9019[1]	2.6697	2.6261[1]	2.6923
2(3402)	6	3.1113[4]	0.9611	1.8532[4]	0.8963
3(3423)	6	3.0093[7]	0.9793	1.7513[7]	1.0068
4(3425)	6	2.9186[8]	0.6833	1.7008[8]	0.7959
5(3451)	4	2.8985[9]	1.3557	1.6392[9]	1.2398
6(3452)	4	3.0153[6]	1.3968	1.7628[6]	1.3685
7(3454)	6	3.1407[3]	1.7949	1.8827[3]	1.7374
8(3455)	6	3.0754[5]	1.2651	1.8214[5]	1.2441
9(3457)	4	3.1920[2]	1.9108	1.9412[2]	1.8623

^athe number of added H or Cl atoms, i. e., the number of pentagon-pentagon fusion vertex (PPFV) for each isomer according to the method we generated the derivatives.

to discuss the relative stability of $C_{64}X_n$, we define C-X bond energy ΔE as follows [24]:

$$\Delta E = \frac{1}{n}(E_{C_{64}} + nE_X - E_{C_{64}X_n})$$

The higher the C-X bond energy ΔE , the greater the stability of $C_{64}X_n$.

Table II lists the B3LYP/6-31G*//B3LYP/6-31G* C-X bond energy ΔE and relative stability, LUMO-HOMO gap energies of the hydro- and chloro- derivatives of nine lowest-energy C_{64} isomers such as $C_{64}X_n$ ($X = H$ or Cl , $n = 4$ or 6). We still use the spiral nomenclature to label the generated fullerene derivatives.

The stability order is changed after H atoms are attached to the C_{64} isomers. As expected, the $C_{64}H_4$ 1911, with a remarkably largest C-H bond energy, turns out to be the most stable in all $C_{64}H_n$ derivatives. The following ones are $C_{64}H_4$ 3457 and $C_{64}H_6$ 3454, both having C_2 symmetry. Derivative 3451, which has been evolved from the ground state of C_{64} isomers, becomes the most instable among the nine derivatives.

Corresponding to its remarkable larger C-X bond energy ΔE , the $C_{64}H_4$ 1911 has the largest LUMO-HOMO gap energy, 2.6697 eV, while that of its parent C_{64} 1911 is only

1.0879 eV. The LUMO-HOMO gap energies of others are also shifted, implying that the chemical deriving on PPFV could affect the electronic structures of non-IPR fullerenes.

Obviously, the chemical deriving on PPFV could indeed enhance the stability of the non-IPR fullerenes in the case from C_{64} 1911 to $C_{64}H_4$ 1911. However, the effects are different for different isomers. It seems that the vertex of the triplet fused pentagons are rather more favorable for hydrogen addition than other types of vertex, which is consistent with the suggestion by Liu *et al.* [25].

The effects of Cl addition are similar to that of the H addition. After Cl atoms attached to the C_{64} isomers, the stability order is changed, and the new order is entirely the same as that of the H addition. $C_{64}Cl_4$ 1911 also becomes the most stable with a remarkable larger C-Cl bond energy. The LUMO-HOMO gap energies are changed with the same manner too. $C_{64}Cl_4$ 1911 also has the highest LUMO-HOMO gap energy, 2.6923 eV, in all $C_{64}Cl_n$ derivatives. These give us a clue that haloid atoms may be appropriate for the chemical deriving on the PPFV of non-IPR fullerenes to stabilize the structure.

Now we attach H, F, Cl, Br atoms to the PPFV of the isomer C_{64} 1911 to construct $C_{64}X_4$ ($X = H, F, Cl, Br$) fullerene derivatives and, to study their structural and electronic properties. Fig. 2 displays the geometrical structures of $C_{64}X_4$ ($X = H, F, Cl, Br$). These molecules like pears in shape with four short hairs on its tapering top or odd pears with four stalks. The tapering top of C_{64} cage is composed of a triplet of directly fused pentagons. Its strain is obviously high due to its high surface curvature, which is a key factor for its instability. The length of C-X bond along the C_3 axis in $C_{64}X_4$ ($X = H, F, Cl, Br$) is about 1.09, 1.36, 1.77, 1.93 Å, respectively, while the length of other C-X ($X = H, F, Cl, Br$) bonds around the C_3 axis is about 1.10, 1.38, 1.82, 1.99 Å, respectively. The bond lengths of C-X bonds along the C_3 axis are nearly the same as the experimental value of C-X ($X = H, Cl, Br$) bond length in methane (CH_4), CF_4 , chloroform (CCl_4) or CBr_4 , while the other bonds around the C_3 axis are somewhat longer. For a comparison, we have tried to put H, F, Cl or Br atom along the C_3 axis into the inner of C_{64} cage, and found that the calculated energies are higher than those when these atoms are added to the outer of the cage, suggesting that the exohedral fullerenes $C_{64}X_4$ ($X = H, F, Cl, Br$) are more stable.

Fig. 2 also show the Mulliken atomic charge populations of $C_{64}X_4$ ($X = H, F, Cl, Br$). The PPFV C atoms (i.e. those bonded with X atoms) in $C_{64}H_4$ are colored in red, indicating that their charges are rather negative. The other atoms at the tapering top of C_{64} cage

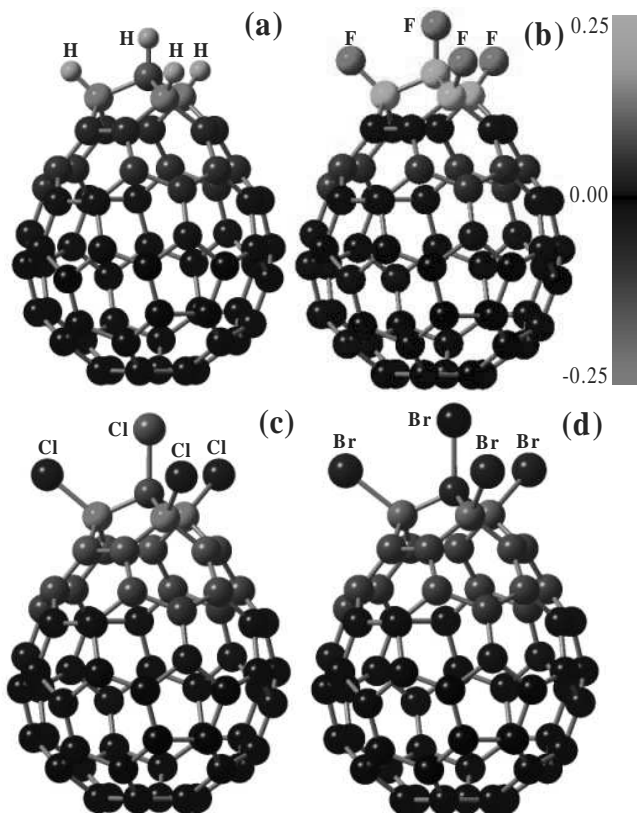


FIG. 2: Schematic structures and Mulliken atomic charge populations of $C_{3v} C_{64}X_4$ molecules: (a) $C_{64}H_4$, (b) $C_{64}F_4$, (c) $C_{64}Cl_4$, and (d) $C_{64}Br_4$. The capital letters indicate the exohedral atoms, and the rest atoms are all C atoms. The color of the atoms show the Mulliken atomic charge amount in electrons.

are marked in dark green, showing that they carry little positive charges. The atoms at bottom are electroneutral as they are in black color. The charge populations of $C_{64}X_4$ ($X = Cl, Br$) are mainly similar to $C_{64}H_4$. The PPFV C atoms in $C_{64}X_4$ ($X = Cl, Br$) are also red, negative charged; while the tapering top of C_{64} cage are dark green, little positive charged. Interestingly, the colors of X atoms (namely light green, dark green, and dark red for $X = H, Cl, Br$, respectively), are quite distinct, revealing that the charge transfers of H, Cl, Br atoms, when fused to the C_{64} cage, are different. The charges of H atoms are rather positive, while those of Cl atoms are less positive, and those of Br atoms are even little negative. With regard to electron transfers, the PPFV C atoms act as electron acceptors, while H and Cl atoms act as electron donors, but Br could not. Surprisingly, the addition of F atoms behaves rather differently. Contrary to $C_{64}X_4$ ($X = H, Cl, Br$), the

PPFV C atoms are positive charged (bright green color) and F atoms are negative charged (light red color), showing a totally inverse electron transfers. All the above results imply that a proper chemical modification on PPFV could change the electronic structures of the non-IPR carbon cage, but adding different atoms would bring different consequences.

For $C_{64}H_4$ and $C_{64}Cl_4$, we have calculated the C-X bond energy ΔE . In the same method, the obtained C-X bond energy ΔE for $C_{64}X_4$ ($X = F, Br$) are 4.2810 eV, 2.4200 eV, respectively. As ΔE of $C_{64}H_4$ is 2.6697 eV, it seems that $C_{64}F_4$ is even more stable than $C_{64}H_4$.

We have also calculated the LUMO-HOMO gap of C_{64} and $C_{64}X_4$ ($X = H, F, Cl, Br$) by B3LYP/6-31G*. The gap of C_{64} is 1.0879 eV, while those of $C_{64}X_4$ are 2.6697 eV, 2.7075 eV, 2.6923 eV, 2.6762 eV for $X = H, F, Cl, Br$, respectively, which is comparable to the gap energy (2.758eV) of C_{60} calculated within the same computational method. A large LUMO-HOMO gap energy has been taken as an indication of a large stability of fullerenes[26, 27]. The remarkable enlargement of the gap energy from C_{64} to $C_{64}X_4$ implies that the chemical deriving could indeed enhance the stability of non-IPR fullerenes.

The DOS provide a convenient overall view of the electronic structure of clusters and solids. Fig. 3 exhibits the DOS of C_{64} and $C_{64}X_4$ ($X = H, F, Cl, Br$), which are obtained by Fermi-Dirac smearing of molecular energy levels. We can see that from C_{64} to $C_{64}X_4$ ($X = H, F, Cl, Br$), LUMO-HOMO gaps are enlarged.

To provide a verifying basis for the experimental identification of $C_{64}X_4$ ($X = H, F, Cl, Br$), we have calculated the IR, Raman spectra by B3LYP/6-31G*, and NMR spectra by GIAO-B3LYP/6-31G*, with the optimized geometry in the B3LYP/6-31G* level, as shown in Figs. 4 and 5.

As can be seen in Figs. 4(a) and 4(b), the computed IR spectrum of $C_{64}H_4$ agrees well with the experimental results[10]; both IR and Raman spectra of $C_{64}H_4$ spread up to more than 3000 cm^{-1} and have two major regions. The region of two sharp peaks near 3000 cm^{-1} corresponds to the C-H stretching modes which are rather active in both IR and Raman spectra, and the wide region in the range less than 1700 cm^{-1} corresponds to the C-C stretching, C-C-C bending and C-C-H bending modes in which active modes are different for IR and Raman spectra.

The IR and Raman spectra of $C_{64}X_4$ ($X = F, Cl, Br$) are rather different, as depicted in Figs. 4(c) to 4(h). Unlike $C_{64}H_4$, they are only extended to circa 1700 cm^{-1} and have no distinct separated regions. From a view of vibrational modes, the spectra of $C_{64}X_4$

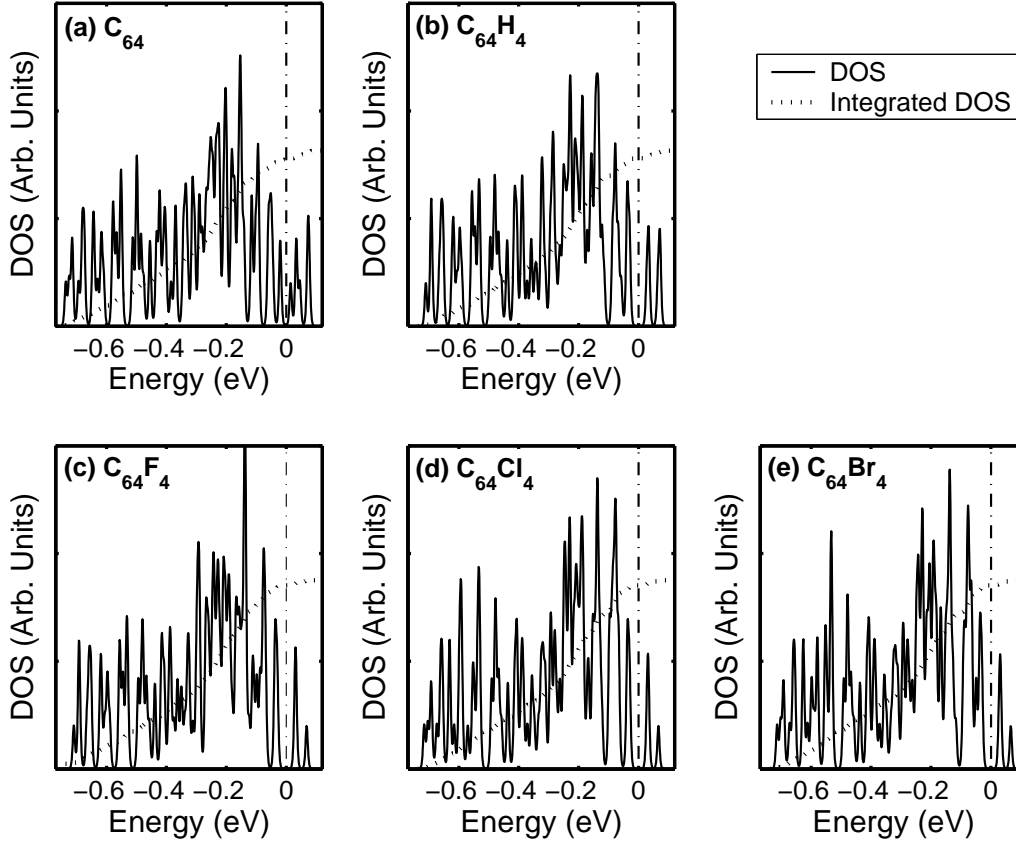


FIG. 3: Density of states (DOS) and the integrated DOS(dotted line) of electrons as a function of energy for C_{64} and $C_{64}X_4$ ($X = H, F, Cl, Br$). The energy zero-point is taken at the Fermi level, that is indicated by the vertical dash-dot line.

($X = F, Cl, Br$) lack a clear region of C-X stretching modes like $C_{64}H_4$. It may be because H atom is much lighter than C atom, the C-H stretching modes could be separated from other modes caused by C atoms, and the corresponding peaks are located at a very high frequency region. By contrast, F, Cl and Br atoms are heavier than C atom, the motion of F, Cl and Br atoms must be coupled with C atoms strongly, resulting in that the IR and Raman spectra of $C_{64}Cl_4$ could not be parted into two regions. This may also cause other spectral differences between $C_{64}H_4$ and $C_{64}Cl_4$.

For $C_{64}X_4$ ($X = F, Cl, Br$), the IR spectra profiles exhibit some similarity, but the main peaks are located at different frequencies. It seems that, from $C_{64}F_4$ to $C_{64}Br_4$, the main peaks of IR spectra are red shifted, and intensities are reduced. Raman spectra show more similarity: not only are the profiles very similar, but also the main peaks are all located between 1400 cm^{-1} and 1600 cm^{-1} . By a careful check, the Raman spectrum of

$C_{64}H_4$ below 1600 cm^{-1} in Fig. 4(b) also presents the above similarity to that of $C_{64}X_4$ ($X = F, Cl, Br$). In addition, the Raman spectral activity grows from $C_{64}H_4$ to $C_{64}Br_4$. We can conclude that the IR spectra are more sensitive to different added X atoms than Raman spectra: the heavier added X atoms will red-shift the main active IR modes and reduce their intensities, but will enhance the activity of Raman modes and not affect the active Raman modes frequencies.

Fig. 5 gives the calculated NMR spectra of $C_{64}X_4$ ($X = H, F, Cl, Br$). The computed NMR spectrum of $C_{64}H_4$ agrees well with the experimental results as depicted in Fig. 4(a). The C_{3v} $C_{64}X_4$ have 14 unique types of C atoms [$60\ sp^2$ C atoms ($8 \times 6; 4 \times 3$); $4\ sp^3$ C atoms ($1 \times 3; 1 \times 1$)] and 2 unique types of X atoms [total 4 X atoms ($1 \times 3; 1 \times 1$)], where $a \times b$ represents a unique types, and in one type, there are b symmetrical equivalent atoms. All of the calculated C^{13} NMR spectra of C atoms in $C_{64}X_4$ ($X = H, F, Cl, Br$) are easily divided into two regions. One may see that there are 12 peaks in the left region, 8 of which have the same intensity, and the other 4 have the half of the intensity, which could be ascribed to the $sp^2(8 \times 6; 4 \times 3)$ C atoms. The right regions of $C_{64}X_4$ ($X = H, F, Cl, Br$) only have two peaks, whose relative intensities are 3:1. It is interesting to note that the two peaks in $C_{64}H_4$ are very close, where the higher peak is in the left, whereas the two peaks in $C_{64}F_4$ are separated from each other, where the higher peak is in the right. We can ascribe this feature to the $sp^3(1 \times 3; 1 \times 1)$ C atoms which are bonded to the X atoms (i.e. PPFV). The lower peak could be ascribed to the single C atom on the C_3 axis, and another peak could be ascribed to the equivalent triple C atoms out of the C_3 axis. The NMR spectra of $C_{64}Cl_4$ and $C_{64}Br_4$ are rather similar to those of $C_{64}F_4$, with small quantitative differences. The calculated H^1 NMR spectrum of H atoms in $C_{64}H_4$ is also included, where the two peaks are observed in an intensity ratio of about 3:1. Obviously, the lower peak can be ascribed to the single H atom on the C_3 axis, whereas another peak can be ascribed to the equivalent triple H atoms out of the C_3 axis.

Let us now address another interesting issue if $C_{64}X_4$ ($X = H, F, Cl, Br$) molecules can condense to form a monolayer structure. We have considered the hexagonal lattice, which has been simulated by a supercell with layer-layer distance of $30\ \text{\AA}$. The $C_{64}X_4$ molecules are put on the lattice site with C_3 axis perpendicular to the monolayer plane. Then, the total energy is calculated accordingly with respect to different lattice parameters (every $0.1\ \text{\AA}$) for the presumed structure. For $C_{64}H_4$ hexagonal monolayer, as indicated in Fig. 6, a clearly

single minimal total energy with the optimized lattice constant $a_0 = 9.89 \text{ \AA}$ is obtained, revealing that this structure is stable and easily to form. The data with 0.01 \AA precision are obtained by a spline interpolation from the calculated data with 0.1 \AA precision. The cohesive energy per $C_{64}H_4$ molecule for this monolayer is found to be 0.48 eV . For $C_{64}X_4$ ($X = F, Cl, Br$), the hexagonal monolayer structure is also found to be stable, and the optimized lattice constants are still $a_0 = 9.89 \text{ \AA}$. The cohesive energy per molecule are 0.67 eV , 0.55 eV , 0.32 eV , respectively. It appears that $C_{64}F_4$ hexagonal monolayer phase is the most stable among them.

To summarize, in terms of first-principles calculations based on the density functional theory, we have systematically reported the structures, electronic properties and spectroscopies of the unconventional fullerene C_{64} and its derivatives $C_{64}X_4$ ($X = H, F, Cl, Br$). We have found that the parent carbon cage of the recently synthesized $C_{64}H_4$ with C_{3v} symmetry is not the ground state of C_{64} , while the latter should be a spherical shaped, D_2 symmetrical isomer with spiral number 3451. Our computation results show that the combination of the four X ($X = H, Cl, F, Br$) atoms to the pentagon-pentagon fusion vertex of C_{64} cage could change the electronic structures and enhance the stability of the fullerenes, and $C_{64}X_4$ ($X = F, Cl, Br$) may be also stable unconventional fullerenes like $C_{64}H_4$. Similar to $C_{64}H_4$, $C_{64}X_4$ ($X = F, Cl, Br$) are found to be pear-shaped, with large LUMO-HOMO gap energies and large C-X bond energy. It appears that $C_{64}F_4$ is even more stable than $C_{64}H_4$ as the C-X bond energy of the former is higher than that of the latter. The computed spectroscopies of $C_{64}H_4$ molecule agree well with the experimental data; the IR, Raman, NMR spectra of $C_{64}X_4$ ($X = F, Cl, Br$) are also presented to stimulate further experimental investigations. In addition, it is revealed that, by total energy calculations, $C_{64}X_4$ could form stable hexagonal monolayers and among them, $C_{64}F_4$ hexagonal monolayer is the most stable.

The authors are grateful to B. Gu, H. F. Mu, and Z. C. Wang for helpful discussions. All of the calculations are completed on the supercomputer NOVASCALE 6800 in Virtual Laboratory of Computational Chemistry, Computer NetWork Information Center (Supercomputing Center) of Chinese Academy of Sciences. This work is supported in part by the National Science Foundation of China (Grant Nos. 90403036, 20490210), and by the MOST of China

(Grant No. 2006CB601102).

- [1] Kroto, H. W.; Heath, J. R.; O'Brien, S. C.; Curl, R. F.; Smalley, R. E. *Nature* **1985**, *318*, 162.
- [2] Kroto, H. W. *Nature* **1987**, *329*, 529.
- [3] Kadish, K. M.; Ruoff, R. S.; Editors, *Fullerene: Chemistry, Physics and Technology*; Wiley: New York, 2002.
- [4] Albertazzi, E.; Domene, C.; Fowler, P. W.; Heine, T.; Seifert, G.; Alsenow, C. V.; Zerbetto, F. *Phys. Chem. Chem. Phys.* **1999**, *1*, 2913.
- [5] Taylor, R.; Avent, A. G.; Birkett, P. R., Dennis, T. J. S.; Hare, J. P.; Hitchcock, P. B.; Holloway, J. H.; Hope, E. G.; Kroto, H. W.; Langley, G. J.; Meidine, M. F.; Parsons, J. P.; Walton, D. R. M. *Pure & Appl. Chem.*, **1993**, *65*, 135.
- [6] Wang, C.-R.; Kai, T.; Tomiyama, T.; Yoshida, T.; Kobayashi, Y.; Nishibori, E.; Takata, M.; Sakata, M.; Shinohara, H. *Nature* **2000**, *408*, 426.
- [7] Stevenson, S.; Fowler, P. W.; Heine, T.; Duchamp, J. C.; Rice, G.; Glass, T.; Harich, K., Hajdu, E.; Bible, R.; Dorn, H. C. *Nature* **2000**, *408*, 427.
- [8] Kato, H.; Taninaka, A.; Sugai, T.; Shinohara, H. *J. Am. Chem. Soc.* **2003**, *125*, 7782.
- [9] Xie, S.-Y.; Gao, F.; Lu, X.; Huang, R.-B.; Wang, C.-R.; Zhang, X.; Liu, M.-L.; Deng, S.-L.; Zheng, L.-S. *Science* **2004**, *304*, 699.
- [10] Wang, C.-R.; Shi, Z.-Q.; Wan, L.-J.; Lu, X.; Dunsch, L.; Shu, C.-Y.; Tang, Y.-L.; Shinohara, H. *J. Am. Chem. Soc.* **2006**, *128*, 6605.
- [11] Yan, Q.-B.; Zheng, Q.-R.; Su, G. *Phys. Rev. B* **2006**, *73*, 165417.
- [12] Fowler, P. W.; Manolopoulos, D. E. *An Atlas of Fullerenes*; Clarendon: Oxford, 1995.
- [13] Dewar, M. J. S.; Thel, W. *J. Am. Chem. Soc.* **1977**, *99*, 4899.
- [14] Chen, Z.; Thiel, W. *Chem. Phys. Lett.* **2003**, *367*, 15.
- [15] Albertazzi, E.; Domene, C.; Fowler, P. W.; Heine, T.; Seifert, G.; Alsenow, C. V.; Zerbetto, F. *Phys. Chem. Chem. Phys.* **1999**, *1*, 2913.
- [16] Hohenberg, P.; Kohn, W. *Phys. Rev.* **1964**, *136*, B864.
- [17] Becke, A. D. *J. Chem. Phys.* **1993**, *98*, 5648.
- [18] Lee, C.; Yang, W.; Parr, R. G. *Phys. Rev. B* **1988**, *37*, 785.

- [19] Gaussian 03, Revision C.02, Frisch, M. J.; Trucks, G. W.; Schlegel, H. B.; Scuseria, G. E.; Robb, M. A.; Cheeseman, J. R.; Montgomery, J. A.; T. Vreven, Jr.; Kudin, K. N.; Burant, J. C.; Millam, J. M.; Iyengar, S. S.; Tomasi, J.; Barone, V.; Mennucci, B.; Cossi, M.; Scalmani, G.; Rega, N.; Petersson, G. A.; Nakatsuji, H.; Hada, M.; Ehara, M.; Toyota, K.; Fukuda, R.; Hasegawa, J.; Ishida, M.; Nakajima, T.; Honda, Y.; Kitao, O.; Nakai, H.; Klene, M.; Li, X.; Knox, J. E.; Hratchian, H. P.; Cross, J. B.; Adamo, C.; Jaramillo, J.; Gomperts, R.; Stratmann, R. E.; Yazyev, O.; Austin, A. J.; Cammi, R.; Pomelli, C.; Ochterski, J. W.; Ayala, P. Y.; Morokuma, K.; Voth, G. A.; Salvador, P.; Dannenberg, J. J.; Zakrzewski, V. G.; Dapprich, S.; Daniels, A. D.; Strain, M. C.; Farkas, O.; Malick, D. K.; Rabuck, A. D.; Raghavachari, K.; Foresman, J. B.; Ortiz, J. V.; Cui, Q.; Baboul, A. G.; Clifford, S.; Cioslowski, J.; Stefanov, B. B.; Liu, G.; Liashenko, A.; Piskorz, P.; Komaromi, I.; Martin, R. L.; Fox, D. J.; Keith, T.; Al-Laham, M. A.; Peng, C. Y.; Nanayakkara, A.; Challacombe, M.; Gill, P. M. W.; Johnson, B.; Chen, W.; Wong, M. W.; Gonzalez, C.; Pople, J. A. Gaussian, Inc., Wallingford CT, 2004.
- [20] The ABINIT code is a common project of the Universite Catholique de Lovain, Corning Incorporated, and other contributors (<http://www.abinit.org>).
- [21] Troullier, N.; Martins, J. L. *Phys. Rev. B* **1991**, *43*, 1993.
- [22] Goedecker, S.; Teter, M.; Hutter, J. *Phys. Rev. B* **1996**, *54*, 1703.
- [23] Lu, X.; Chen, Z.; Thiel, W.; Schleyer, P. von R.; Huang, R.; Zheng, L. *J. Am. Chem. Soc.* **2004**, *126*, 14871.
- [24] Chiu, Y. N.; Ganelin, P.; Jiang, X.; Wang, B. C.; *J. Mol. Struct. (Theochem)* **1994**, *312*, 215.
- [25] Liu, M.; Chiu, Y.-N.; Xiao, J. *J. Mol. Struct. (Theochem)* **1999**, *489*, 109.
- [26] Manopoulos, D. E.; May, J. C.; Down, S. E.; *Chem. Phys. Lett.* **1991**, *181*, 105.
- [27] Diener, M. D.; Alford, J. M. *Nature* **1998**, *393*, 668.

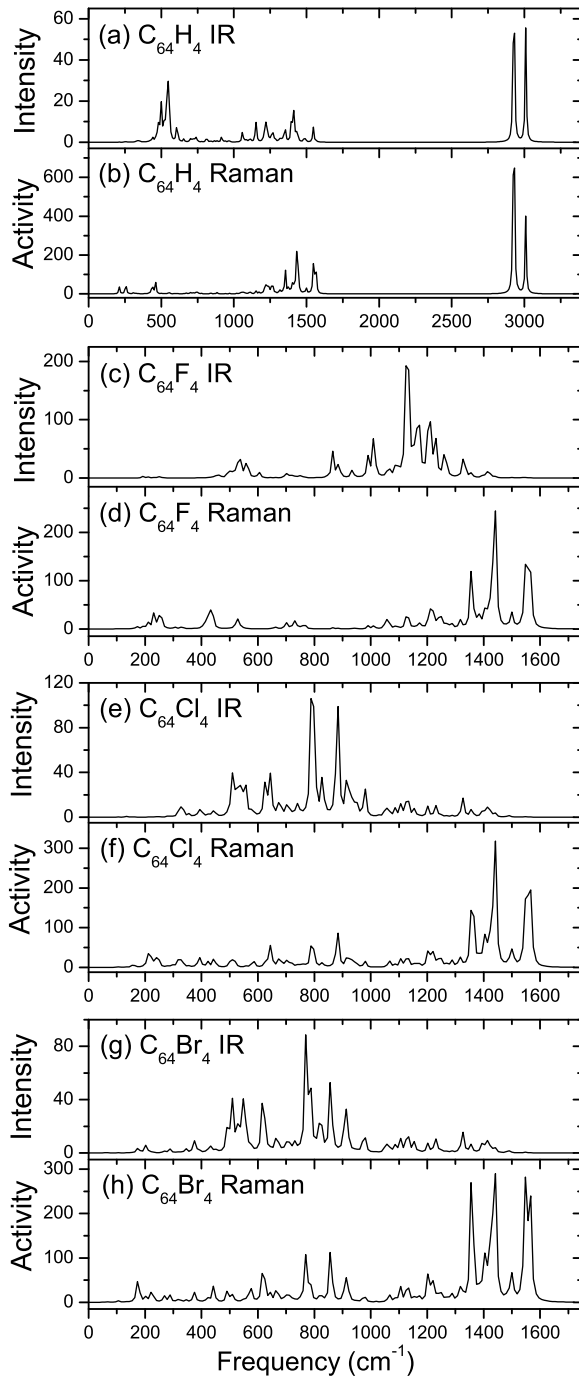


FIG. 4: IR and Raman spectra of $C_{3v} C_{64}X_4$ ($X=H, F, Cl, Br$), which are scaled by a factor of 0.9613.

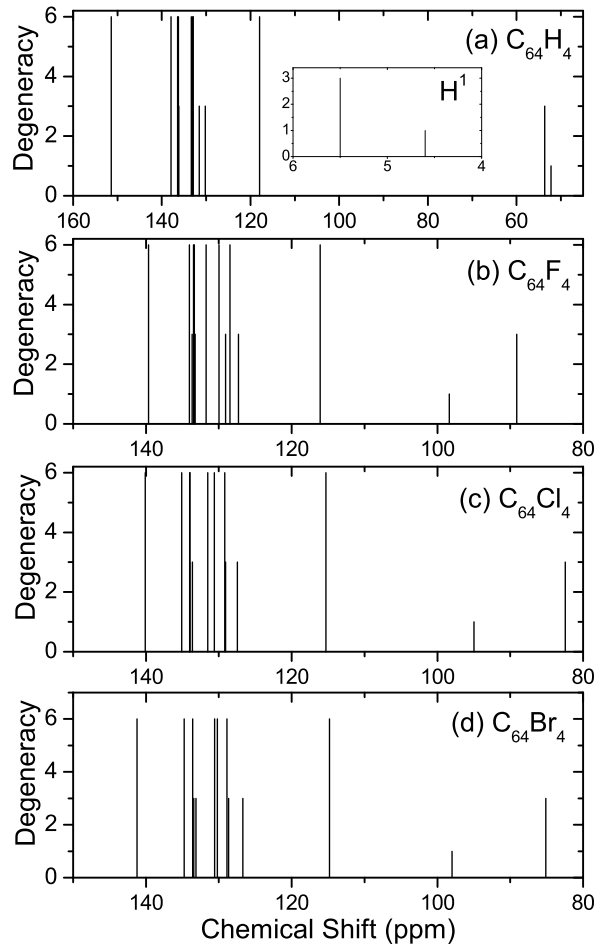


FIG. 5: NMR spectra of $C_{3v} C_{64}X_4$ ($X = H, F, Cl, Br$), scaled by referenced shifts, where the inset of (a) shows the chemical shifts of H atoms, others show that of C atoms.

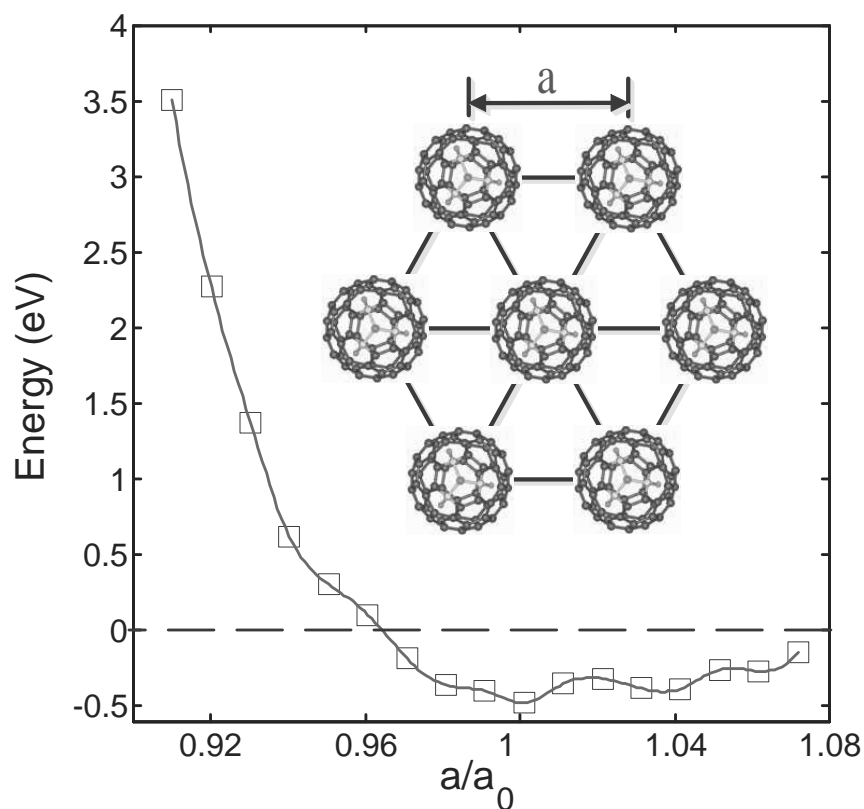


FIG. 6: The total energy per $C_{64}H_4$ molecule in hexagonal monolayer, measured from the total energy of the isolated $C_{64}H_4$ molecule, as a function of the lattice constant, where the optimized lattice constant, $a_0 = 9.89 \text{ \AA}$.